9-1-2009

Loss of Halophytism by interference with SOS1 expression

Dong Ha Oh
University of Illinois at Urbana-Champaign

Eduardo Leidi
CSIC - Instituto de Recursos Naturales y Agrobiologia de Sevilla (IRNAS)

Quan Zhang
Shandong Normal University

Sung Min Hwang
Gyeongsang National University

Youzhi Li
Guangxi University

See next page for additional authors

Recommended Citation

Oh, D., Leidi, E., Zhang, Q., Hwang, S., Li, Y., Quintero, F., Jiang, X., D'urzo, M., Lee, S., Zhao, Y., Bahk, J., Bressan, R., Yun, D., Pardo, J., & Bohnert, H. (2009). Loss of Halophytism by interference with SOS1 expression. *Plant Physiology, 151* (1), 210-222. https://doi.org/10.1104/pp.109.137802

Loss of Halophytism by Interference with SOS1 Expression[1][W][OA]

Dong-Ha Oh, Eduardo Leidi, Quan Zhang, Sung-Min Hwang, Youzhi Li, Francisco J. Quintero, Xingyu Jiang, Matilde Paino D'Urzo, Sang Yeol Lee, Yanxiu Zhao, Jeong Dong Bahk, Ray A. Bressan, Dae-Jin Yun, José M. Pardo, and Hans J. Bohnert*

Departments of Plant Biology and Crop Sciences, University of Illinois at Urbana-Champaign, Urbana, Illinois 61801 (D.-H.O., Q.Z., Y.L., H.J.B.); Division of Applied Life Science (BK21 Program) and Environmental Biotechnology National Core Research Center, Graduate School of Gyeongsang National University, Jinju 660–701, Korea (D.-H.O., S.-M.H., S.Y.L., J.D.B., D.-J.Y.); Instituto de Recursos Naturales y Agrobiología, Consejo Superior de Investigaciones Científicas, Seville 41012, Spain (E.L., F.J.Q., X.J., J.M.P.), Key Laboratory of Plant Stress Research, College of Life Science, Shandong Normal University, Jinan 250014, China (Q.Z., Y.Z.); Key Laboratory of Ministry of Education for Microbial and Plant Genetic Engineering, Guangxi University, Nanning, Guangxi 530005, China (Y.L.); and Department of Horticulture and Landscape Architecture, Purdue University, West Lafayette, Indiana 47907 (M.P.D., R.A.B.)

The contribution of SOS1 (for Salt Overly Sensitive 1), encoding a sodium/proton antiporter, to plant salinity tolerance was analyzed in wild-type and RNA interference (RNAi) lines of the halophytic Arabidopsis (*Arabidopsis thaliana*)-relative *Thellungiella salsuginea*. Under all conditions, *SOS1* mRNA abundance was higher in *Thellungiella* than in Arabidopsis. Ectopic expression of the *Thellungiella* homolog ThSOS1 suppressed the salt-sensitive phenotype of a *Saccharomyces cerevisiae* strain lacking sodium ion (Na^+) efflux transporters and increased salt tolerance of wild-type Arabidopsis. *thsos1*-RNAi lines of *Thellungiella* were highly salt sensitive. A representative line, *thsos1-4*, showed faster Na^+ accumulation, more severe water loss in shoots under salt stress, and slower removal of Na^+ from the root after removal of stress compared with the wild type. *thsos1-4* showed drastically higher sodium-specific fluorescence visualized by CoroNa-Green, a sodium-specific fluorophore, than the wild type, inhibition of endocytosis in root tip cells, and cell death in the adjacent elongation zone. After prolonged stress, Na^+ accumulated inside the pericycle in *thsos1-4*, while sodium was confined in vacuoles of epidermis and cortex cells in the wild type. RNAi-based interference of *SOS1* caused cell death in the root elongation zone, accompanied by fragmentation of vacuoles, inhibition of endocytosis, and apoplastic sodium influx into the stele and hence the shoot. Reduction in SOS1 expression changed *Thellungiella* that normally can grow in seawater-strength sodium chloride solutions into a plant as sensitive to Na^+ as Arabidopsis.

Accompanying the production and accumulation of osmolytes and other protective molecules, an important aspect of plant responses leading to salt stress tolerance is the regulation of uptake, reexport, and control over the distribution of sodium ions (Na^+; Hasegawa et al., 2000; Tester and Davenport, 2003). Na^+ appear to enter the root by several pathways (Essah et al., 2003; Pardo et al., 2006), although the nature of participating genes and their interaction in pathways require further investigation. Once Na^+ has entered the root endodermis, a tissue that represents a barrier to ions (Peng et al., 2004), it is generally assumed that the ion enters the xylem following the movement of water to aerial parts of the plant. Despite substantial efflux of Na^+ across the plasma membrane of root cells, the net flux of Na^+ is unidirectional from soil to roots and then to the shoot, except for possible recirculation via the phloem (Tester and Davenport, 2003). In a range of species, the severity of damaging symptoms is positively correlated with the content of Na^+ reaching photosynthetic tissues (Davenport et al., 2005; Ren et al., 2005; Munns et al., 2006). However, halophytic species can accumulate very high amounts of Na^+ in vacuoles, such that Na^+ may account for most of the total cellular osmotic potential (Tester and Davenport,

[1] This work was supported by the World Class University Program (grant no. R32–10148), the Environmental Biotechnology National Core Research Center Project (grant no. R15–2003–012–01002–00), the Biogreen 21 Project of the Rural Development Administration (grant no. 20070301034030), the National Science Foundation (grant no. DBI–0223905), University of Illinois at Urbana-Champaign and Purdue University institutional funds, the Spanish Ministerio de Ciencia e Innovacion (grant no. BFU2006–06968), and the Brain Korea 21 Program (scholarships to S.-M.H.).

* Corresponding author; e-mail hbohnert@illinois.edu.

The author responsible for distribution of materials integral to the findings presented in this article in accordance with the policy described in the Instructions for Authors (www.plantphysiol.org) is: Hans J. Bohnert (hbohnert@illinois.edu).

[W] The online version of this article contains Web-only data.

[OA] Open Access articles can be viewed online without a subscription.

www.plantphysiol.org/cgi/doi/10.1104/pp.109.137802

2003), and the presence of Na^+ accelerates growth in euhalophytes to some degree (Adams et al., 1998). Emerging as the major advantage of halophytes appears to be their exceptional control over Na^+ influx combined with export mechanisms, the ability to coordinate its distribution to various tissues, and efficient sequestration of Na^+ into vacuoles. These characteristics are of particular advantage when plants are subjected to a sudden increase of Na^+ salts in their environment (Hasegawa et al., 2000), whereas gradual increases in Na^+ may be tolerated even by plants that are not halophytic in nature.

Na^+-ATPases, major Na^+ export systems in organisms such as fungi and the moss *Physcomitrella patens*, have not been found in higher plants (Lunde et al., 2007). In Arabidopsis (*Arabidopsis thaliana*), transporters of monovalent (alkali) cations, such as HKT1 (Berthomieu et al., 2003; Rus et al., 2004), members of the NHX family (Yamaguchi et al., 2005; Pardo et al., 2006), and SOS1 (for Salt Overly Sensitive 1; Shi et al., 2000, 2002, 2003), have been shown to play roles in the movement and distribution of Na^+ ions. Studies have shown the involvement of nonselective ion channels with roles in the transport of Na^+ ions, but the genes encoding such function(s) have not been identified (Demidchik and Maathuis, 2007). *SOS1*, whose deletion resulted in a strong salt-sensitivity phenotype in Arabidopsis, encodes a plasma membrane Na^+/H^+ antiporter involved in removing Na^+ ions from cells (Shi et al., 2000). This efflux strategy, which may be sufficient for the survival of unicellular organisms, must be accompanied by other means of Na^+ confinement to avoid carryover of Na^+ between cells in futile cycles. Hence, the physiological role of a plasma membrane Na^+/H^+ antiporter must be embedded in the context of tissue, organ, and whole plant distribution of ions and their transporters. A recent discovery on cell layer-specific differential responses to the salt stress of root cells supported this notion (Dinneny et al., 2008).

In Arabidopsis, the *SOS1* gene is most strongly expressed in the epidermis of the root tip region and in cells adjacent to vascular tissues (Shi et al., 2002). Based on the salt concentration in shoot, root, and xylem sap of wild-type Arabidopsis and its *sos1* knockout mutants, the SOS1 antiporter is assumed to function in Na^+ export under severe salt stress conditions (Shi et al., 2002). However, detailed knowledge about how a Na^+ excluder achieves salt tolerance in a multicellular eukaryote is still missing. Significantly also, even though SOS1 has been an intensely studied component of the ion homeostasis mechanism, its involvement in the exceptional salt tolerance of halophytes is not known.

Thellungiella salsuginea (salt cress), which had before been called *T. halophila* by us, is a close relative of Arabidopsis, which has become a model to study the genetic basis of this plant's extreme tolerance to a variety of abiotic stress factors, including salinity (Inan et al., 2004; Gong et al., 2005; Vera-Estrella et al., 2005; Volkov and Amtmann, 2006; Amtmann, 2009). *Thellungiella* lacks specialized morphological structures, such as salt glands or large sodium storage cells found in other halophytes, making it a useful model for studying stress tolerance mechanisms that could be applicable to further understanding or to embark on engineering of conventional crops (Inan et al., 2004). Recently, it has been reported that *Thellungiella* had lower net Na^+ uptake compared with Arabidopsis. The unidirectional influx of Na^+ ions to roots appeared to be more restricted and/or tightly controlled in *Thellungiella* than in Arabidopsis. To compensate for greater influx, Arabidopsis roots showed higher Na^+ efflux (Wang et al., 2006).

Here, we wished to explore the role(s) by which *ThSOS1*, the *SOS1* homolog in *Thellungiella*, could be involved in shaping the halophytic character of the species using ectopic expression of the gene in yeast and in Arabidopsis and *Thellungiella* SOS1-RNA interference (RNAi) lines. The results identified *ThSOS1* as a genetic element whose activity limits Na^+ accumulation and affects the distribution of Na^+ ions at high concentration, thus acting as a major tolerance determinant.

RESULTS

Thellungiella Expresses *SOS1* at Higher Levels Than Arabidopsis

ThSOS1 (EF207775) is most closely related to Arabidopsis *SOS1* (*AtSOS1*; At2g01980) in the deduced amino acid sequences (83% identity) among *SOS1* coding regions from other plants (Supplemental Fig. S1). *ThSOS1* exists as a single-copy gene in the *Thellungiella* genome (data not shown). Transcript abundance of SOS1 was compared between Arabidopsis and *Thellungiella* by reverse transcription (RT)-PCR. Reference genes were selected among genes more than 90% identical in their sequence identities between both species, while they showed unaltered expression levels under stress conditions (Czechowski et al., 2005). All primers were designed to be identical in both species. In *Thellungiella*, SOS1 mRNA was significantly more abundant than in Arabidopsis in both shoot and root, more prominently expressed in roots in the absence of salt stress, while the levels of reference gene expression were indistinguishable between the two species (Fig. 1A). *SOS1* mRNA was quantified by real-time RT-PCR (Fig. 1B). Compared with wild-type Arabidopsis, *ThSOS1* mRNA abundance was 2.9- and 7.6-fold higher under normal conditions in shoot and root, respectively, and up to 5.7-fold higher compared with salt-stressed Arabidopsis roots under stressed conditions. This difference in *SOS1* mRNAs in both species persisted in older plants of similar mass and growth stages grown on artificial soil as described (Gong et al., 2005) under either nonsalinized or highly saline conditions (Supplemental Fig. S2).

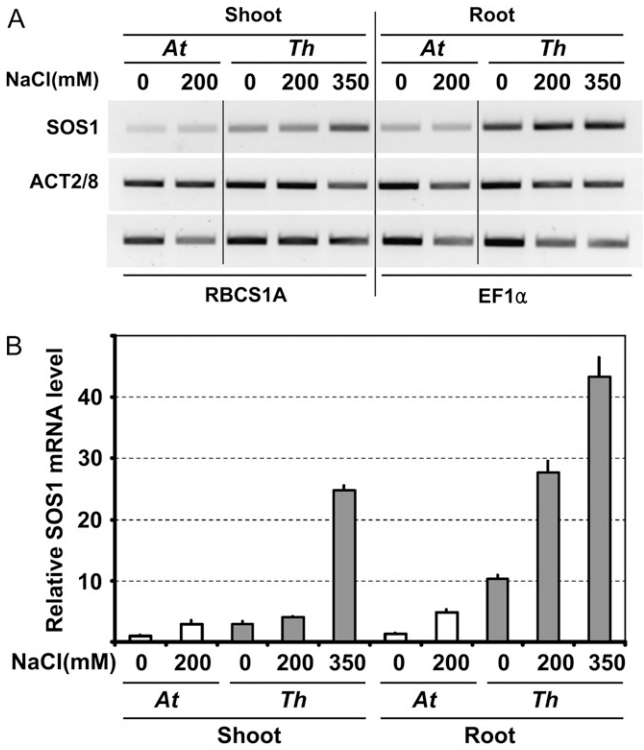

Figure 1. Transcript abundance of SOS1 in Arabidopsis (*At*) and *Thellungiella* (*Th*). A, Transcript abundance was compared by semi-quantitative RT-PCR between Arabidopsis and *Thellungiella* for SOS1. Actin (ACT2/8), ribulose-bisP carboxylase small chain 1A (RBCS1A), and elongation factor 1-α (EF1α) were used as references (Czechowski et al., 2005). Treatment of 350 mM NaCl to Arabidopsis was not included because this stress condition is lethal. B, Quantification of SOS1 transcripts by real-time RT-PCR with error bars indicating SD from six repeats. All primers were designed against regions where the genes of the two species showed perfect identity to generate amplicons of identical length with more than 95% sequence identity between the two species.

ThSOS1 Expression Suppressed the Salt-Sensitive Phenotype of a Yeast Strain Lacking Na^+ Transporters and Increased the Salt Tolerance in Arabidopsis

The *Saccharomyces cerevisiae* strain AXT3K (*Δena1-4 Δnha1 Δnhx1*), lacking major Na^+ transporters essential for tolerance of yeast, showed growth inhibition at Na^+ concentrations higher than 50 mM, while the wild type was not affected (Quintero et al., 2002). Expression of *ThSOS1* partially suppressed the salt sensitivity of AXT3K (Fig. 2A). In Arabidopsis, *AtSOS1* is activated by the SOS2/SOS3 protein kinase complex (Qiu et al., 2002; Quintero et al., 2002). Coexpression of Arabidopsis *SOS2* and *SOS3* in AXT3K together with *ThSOS1* dramatically increased the salt tolerance of the transformed cells, leading to growth in medium with 400 mM sodium (Fig. 2B). Expression of *ThSOS1* conferred salt tolerance to the yeast mutant at concentrations higher than those sustained by the expression of *AtSOS1*, both alone and after activation by SOS2/SOS3 (Fig. 2, A and B). To test whether the unequal Na^+ tolerance was related to differential activity of AtSOS1 and ThSOS1, the Na^+/H^+ exchange activity was measured in plasma membrane vesicles purified by two-phase partitioning from yeast transformants (Fig. 2C). The strong inhibition (approximately 84%) of ATP hydrolysis by vanadate, an inhibitor of plasma membrane H^+-ATPases, demonstrated that vesicle preparations were enriched in plasma membranes (data not shown). Cells were grown on selective Arg-phosphate medium containing 1 mM KCl and transferred to the same medium supplemented with 100 mM NaCl for 1 h to ensure activation of the SOS2/SOS3 kinase complex when present. Maximal Na^+/H^+ exchange activity was observed in cells coexpressing SOS1 proteins and the Arabidopsis SOS2/SOS3 kinase complex (Fig. 2D). No significant differences were found in the Na^+/H^+ exchange activity of plasma membrane vesicles containing ThSOS1 or AtSOS1 with and without coexpression of the SOS2/SOS3 kinase complex (Fig. 2D; data not shown).

Transgenic Arabidopsis expressing *ThSOS1* under control of the cauliflower mosaic virus-35S promoter were analyzed together with *AtSOS1*-overexpressing lines (Shi et al., 2003) for *SOS1* expression and salt tolerance (Fig. 3). The transgenic lines showed various levels of *SOS1* expression, highest in a *ThSOS1*-overexpressing line (Fig. 3A, line 30). The survival rates of the wild type and SOS1-overexpressing lines were quantified by rescuing the seedlings onto nonsaline medium after a brief stress. Seedlings that resumed growth were counted as survivors (Fig. 3B). The survival rates of SOS1-overexpressing lines were proportional to the level of SOS1 under stress (r^2 = 0.95), regardless of SOS1 origin, indicating that expression strength/mRNA stability or protein amount/activity are determining factors in tolerance acquisition. However, even the highest tolerance observed in line 30 (Fig. 3B) did not approach that shown by wild-type *Thellungiella* (Inan et al., 2004).

RNAi-Based Reduction of *ThSOS1* Expression Resulted in Decreased Salt Tolerance with Faster Na^+ Accumulation in Shoots

We have developed transgenic *Thellungiella* transformed with a *ThSOS1* RNAi vector (Fig. 4A). Two lines, designated *thsos1-4* and *thsos1-6*, were used for further analyses. Both showed 3:1 segregation in BASTA resistance and salt sensitivity, indicating a single insertion locus of the RNAi construct (data not shown).

Seedlings on plates (Fig. 4B) and mature plants grown in artificial soil (Supplemental Fig. S3A) showed a salt-sensitive phenotype in the RNAi lines. Shoots of RNAi line plants showed partial bleaching and root growth stopped at 200 mM NaCl, while the wild type and vector control (*thsos1-11*) continued to grow without symptoms in NaCl solutions up to 300 mM (Fig. 4, B and C). The abundance of *ThSOS1* mRNA was determined by quantitative real-time

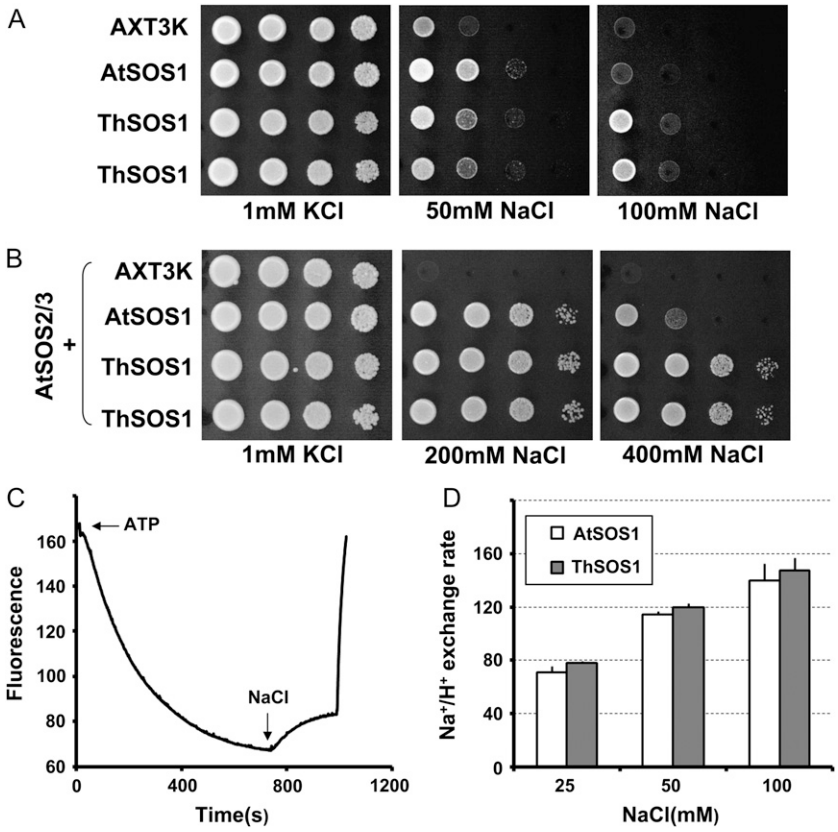

Figure 2. Complementation of the yeast AXT3K mutant with ThSOS1. A, The yeast strain AXT3K (Δ*ena1-4* Δ*nha1* Δ*nhx1*) transformed with either AtSOS1 or ThSOS1 was grown on medium supplemented with the designated concentrations of salt. B, Coexpression of AtSOS1 or ThSOS1 with Arabidopsis SOS2 and SOS3. C, Na^+/H^+ exchange activity in plasma membrane vesicles. Formation of pH gradient, acidic inside, was initiated with ATP. Addition of NaCl started Na^+/H^+ exchange and fluorescence recovery. The reaction was terminated by adding 25 mM $(NH_4)_2SO_4$, which dissipated the pH gradient. One representative experiment is shown. D, Initial rates of Na^+/H^+ exchange (means and SE; $n = 3$); units are percentage change of fluorescence (ΔF) per minute and per milligram of protein.

PCR in roots and shoots with or without salt stress. The decline of *SOS1* mRNA by RNAi was more prominent under salt stress, where *thsos1-4* showed 30% and 84% and *thsos1-6* showed 17% and 40% of wild-type expression in the shoot and root, respectively (Fig. 4D). A similar reduction in *SOS1* transcript amount persisted throughout development and at different strengths of NaCl (Supplemental Figs. S3B and S5). The vector control (*thsos1-11*) showed no significant difference in *ThSOS1* expression from the wild type (data not shown).

To further characterize the role of ThSOS1 in the stress response, 2-week-old plants of wild type and *thsos1-4* were transferred to 200 mM NaCl and fresh weight and water and ion contents of shoots were measured, using inductively coupled plasma-optical emission spectrometry. Wild-type shoots continued to gain weight, but *thsos1-4* shoots showed no growth after day 4 (Fig. 5A). Water content was deduced from a comparison of the fresh and dry weights of seedling shoots. Salt-stressed wild-type shoots maintained water content slightly lower than the unstressed control throughout the experiments. However, a more significant decrease in water content in *thsos1-4* shoots became apparent after 7 d (Fig. 5B). In contrast to the wild type, which showed a linear, gradual increase of Na^+ in the leaves, sodium content in *thsos1-4* leaves peaked by day 4 and later declined, most probably by leakage due to the loss of water (Fig. 5C). Loss of potassium was observed in both the wild type and *thsos1-4*, with a seemingly insignificant higher decrease in *thsos1-4* during later times of the experiment (Fig. 5D). These results already pointed to *ThSOS1* as important and required for the ability to tolerate extremely high levels of NaCl.

The changes in ion content of stressed plants after removal of the stress were compared between the wild type and *thsos1-4* (Fig. 6). Hydroponically grown plants were treated by increasing NaCl stepwise to the nonlethal concentration of 150 mM within 2 weeks, transferred to medium without NaCl, and harvested to determine Na^+ and K^+ concentrations. Both shoots and roots of *thsos1-4* showed higher Na^+ (Fig. 6, A and C) and lower K^+ (Fig. 6, B and D) contents compared with the wild type. In the wild type, shoot ion contents did not change over a 72-h period after removal of the plants from NaCl solutions, while *thsos1-4* showed gradual decreases in Na^+ and increases in K^+, eventually converging on the Na^+ contents observed in the wild type (Fig. 6, A and B). The roots of wild-type plants exhibited a sharp drop in Na^+ ion content within 1 h after removal of NaCl, while the efflux of Na^+ ions was much slower in *thsos1-4* roots, which failed to reach the level of Na^+ content in the wild type at 72 h (Fig. 6C). To assess the contribution of ThSOS1 to the reduction of net sodium uptake in the short term, wild-type and *thsos1-4* plants were transferred to hydroponic medium supplemented with 0.1, 1, and 10

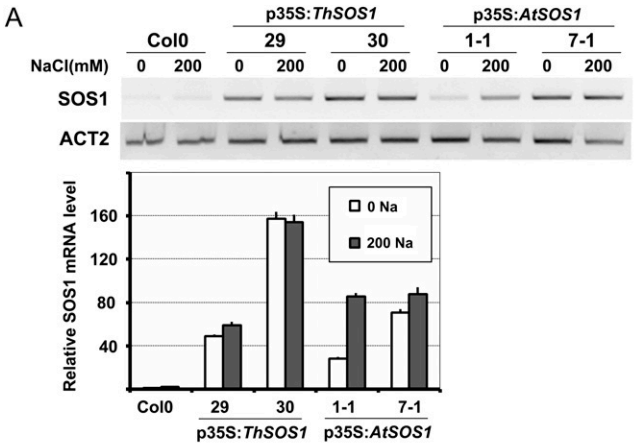

B

Line	Survival rate (%)*
Col	9.8 ± 9.5
29	61.8** ± 6.9
30	98.0 ± 2.7
1-1	67.1** ± 8.1
7-1	64.5** ± 5.3

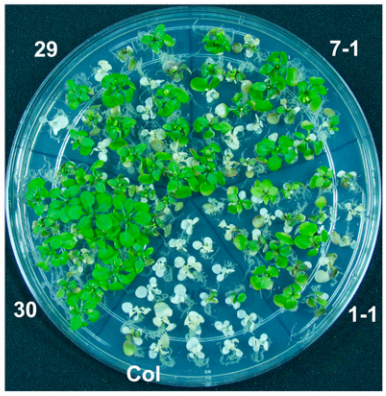

Figure 3. Ectopic expression of *ThSOS1* in Arabidopsis. A, Comparison of *SOS1* mRNA abundance between Arabidopsis wild type (Col0) and representative transgenic lines expressing *ThSOS1* (lines 29 and 30) and *AtSOS1* (lines 1-1 and 7-1) by RT-PCR and quantitative RT-PCR. Error bars represent SD of four independent experiments. B, Salt tolerance phenotypes of the transgenic plants. Seedlings with two true leaves were incubated for 7 d in medium containing 200 mM NaCl and subsequently rescued to medium without NaCl. The photograph shown was taken 5 d after the rescue. *, Percentages of seedlings that produced new leaves. Results are from five biological repeats ($n = 20$ in each repeat). **, Statistically similar at $P < 0.01$ (Tukey test).

mM and the Na^+ content was determined after 15 and 30 min and 2 and 48 h. Roots of line *thsos1-4* started to show significantly greater Na^+ contents than the wild type after 2 h of salt imposition (Supplemental Fig. S4).

Down-Regulation of *ThSOS1* Resulted in Increased Sodium Accumulation in the Root Tip and Cell Death in the Elongation Zone

To determine the role of *ThSOS1* in specific cell types in the roots, the distribution of sodium was imaged using the fluorescent, sodium-specific dye CoroNa-Green AM (Invitrogen), as outlined in "Materials and Methods," comparing wild-type and *thsos1-4* seedling roots by confocal microscopy. Incubations in 150 mM NaCl did not result in rapid differences between the wild type and *thsos1-4*, but within 24 h *thsos1-4* roots showed higher fluorescence in the meristematic region than the wild type (Fig. 7, A and B). When the vacuolar fluorescence intensities of root cortex cells from five individual plants from each line were quantified, the wild type showed a mean relative value of fluorescence intensity of 29.68 (SD = 9.43; arbitrary units), while the mean was 68.80 (SD = 16.89) for *thsos1-4* (Fig. 7C).

Cellular events in the root tip region at this time point were observed by CoroNa Green AM and FM4-64 (Invitrogen). In the wild type, CoroNa Green specifically stained the prevacuolar compartment of irregular shape in the meristematic and expanding cells (Fig. 7D). Cells of *thsos1-4* showed significantly stronger CoroNa-Green fluorescence in small round intracellular vacuoles, which converged into one or two large bodies within 24 h in medium with 150 mM NaCl (Fig. 7E). Interestingly, the endocytotic inclusion of the FM4-64 dye, which was apparent in the wild type (Fig. 7D, arrows in inset), was absent in *thsos1-4* root cells (Fig. 7E, inset). Neither the shape of vacuoles nor endocytosis was affected under normal conditions in the wild type or *thsos1-4* (data not shown).

Whereas wild-type plants did not show any symptoms even during longer term exposure to salt (Fig. 7F), increasing Na^+-specific fluorescence in *thsos1-4* was followed by cell death within and adjacent to the elongation zone, visualized by intracellular staining of propidium iodide (Fig. 7G, arrow). The number of *thsos1-4* seedlings showing higher fluorescence and/or cell death at the root tip and elongation zone increased to two-third of the tested seedlings (10 of 15) within 36 h of stress, and the primary root of all *thsos1-4* seedlings (10 of 10) had died within 48 h.

thsos1-4 Accumulated Sodium in the Root Stele after Long-Term Stress

To visualize Na^+ distribution in the stele, wild-type and *thsos1-4* seedlings were incubated for longer times at low concentrations of CoroNa Green (see "Materials and Methods"). Fluorescein diacetate was used as a control in separate experiments to ensure that dyes penetrated to the vasculature (data not shown). In the wild type, Na^+ was confined in the vacuoles of epidermis, cortex, and, less pronounced, endodermis cells, and fluorescence was absent from pericycle cells and cells within the vasculature after treatment with 150 mM NaCl for up to 4 d (Fig. 8, A, B, E, G, and I). In contrast, cell damage in the elongation zone in *thsos1-4* extended to the older sections of the root as the stress continued (Fig. 8, C and D), resulting in compromised cells with intensive intracellular staining of propidium iodide (Fig. 8F, arrow 1). Strongest CoroNa Green fluorescence was observed in cells adjacent to structurally compromised cells (Fig. 8F, arrow 2). While epidermis and cortex cells were either terminally damaged or failed to confine Na^+ to vacuoles, the Na^+-specific fluorescence was also found in cells inside the pericycle (Fig. 8H, arrows). Within 4 d of incubation, pericycle

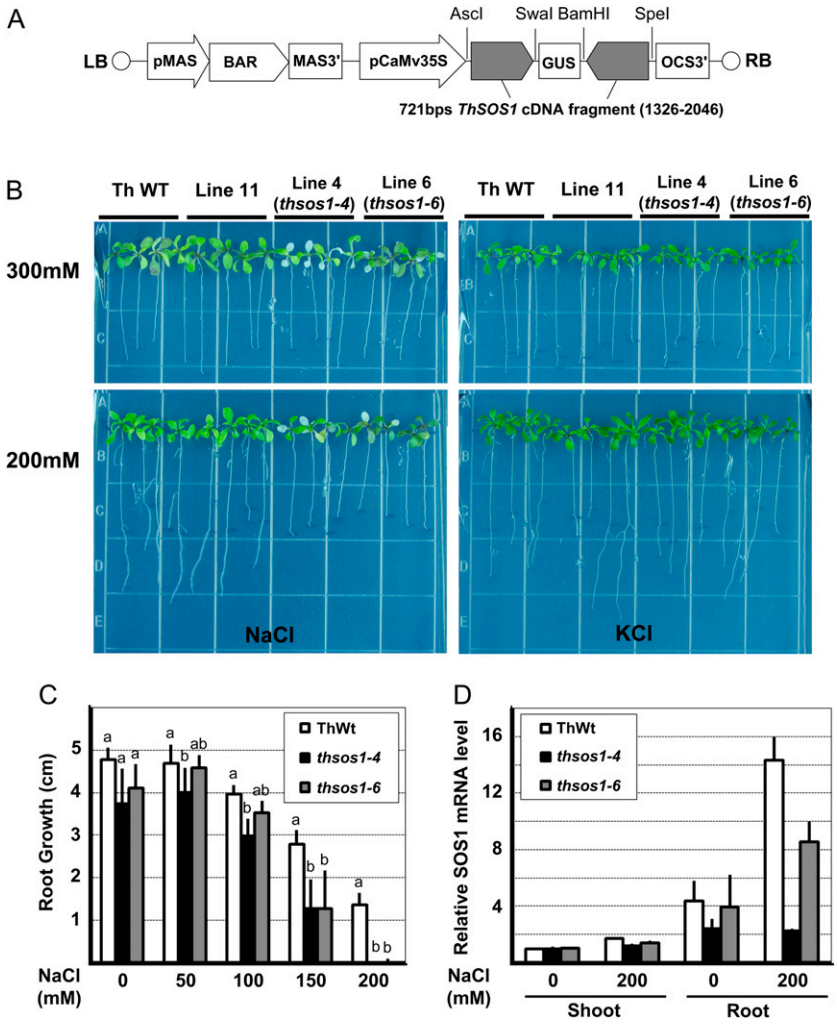

Figure 4. Phenotypes of *ThSOS1*-RNAi plants under salt stress. A, Schematic representation of the vector for RNAi expression. LB, Left border; RB, right border. B, Ten-day-old seedlings incubated vertically for 8 d in the presence of salt. Line 11 constituted a vector control. WT, Wild type. C, Root growth during 8 d of incubation in NaCl concentration as indicated. Error bars indicate SD of nine to 12 seedlings. Within each concentration, bars with different letters are significantly different at $P < 0.01$ (Tukey test). D, SOS1 expression in 3-weeks-old plants determined by quantitative RT-PCR with actin as a control. Error bars indicate SD of six repeats.

cells revealed damage and CoroNa Green stained xylem vessels (Fig. 8J) in *thsos1-4* at the low concentration of NaCl (150 mM), which was not recognized in wild-type plants as a stressful condition, as shown in Figure 8I and also suggested by microarray experiments (Gong et al., 2005).

The higher accumulation of Na^+ ions inside the endodermis of *thsos1-4* was confirmed by scanning electron microscopy and energy-dispersive x-ray microanalysis (SEM-EDX) in the roots of mature plants (Fig. 9). After treatment with 250 mM NaCl for 2 d, *thsos1-4* root accumulated more than twice the amount of Na^+ than wild-type root, concurrent with a dramatic decrease of K^+ in the vacuole of xylem parenchyma that resulted in a more than 12 times higher Na^+-K^+ ratio. In contrast, cortex cells did not show a significant difference between the wild type and *thsos1-4*.

DISCUSSION

In Arabidopsis, the SOS pathway has been documented as an essential component of the ion homeostasis system. The known signal transduction components of the pathway, a complex of SOS2 and SOS3, control the activity of SOS1, a plasma membrane-localized Na^+/H^+ antiporter (Qiu et al., 2002; Quintero et al., 2002; Chinnusamy et al., 2006). The importance of this mechanism in the glycophyte Arabidopsis notwithstanding (Shi et al., 2002, 2003), questions remained about the relative impact of this pathway in a naturally salt-tolerant species. We used the halophytic Arabidopsis relative *Thellungiella* (Bressan et al., 2001) to address this question.

SOS1 Abundance Determines the Extent of Shoot Na^+ Accumulation

While the sequence of SOS1 is highly conserved between *Thellungiella* and Arabidopsis (Oh et al., 2007), a conspicuous difference emerged from comparisons of expression strength: transcript levels in *Thellungiella* were eight to 10 times higher in both nonsalinized and stressed states, and the salt-dependent induction of expression or stabilization *SOS1* mRNA (Chung et al., 2008) known for Arabidopsis

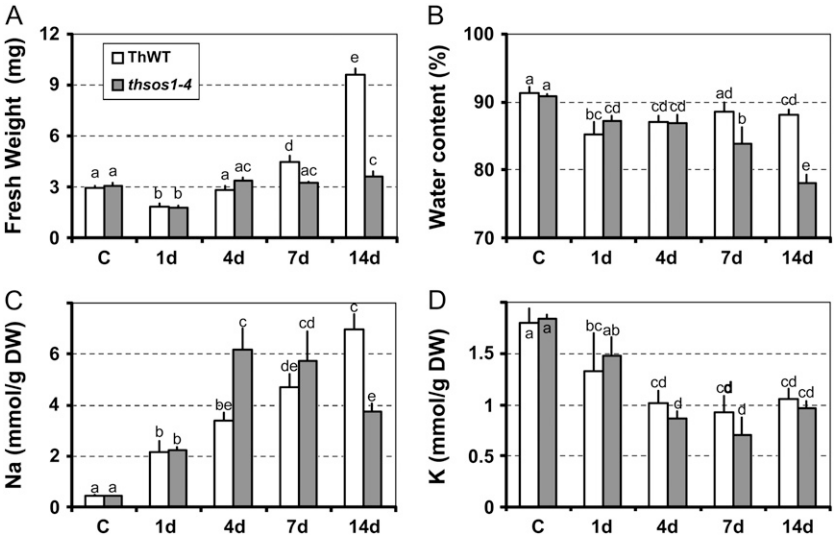

Figure 5. Growth, water, and ion contents of wild-type (WT) and *thsos1-4* seedling shoots. Shoots of seven seedlings grown in the presence of 200 mM NaCl were pooled. The control (C) was from seedlings incubated for 4 d without salt stress. Error bars indicate SD of four independent replicates. Bars with different letters are significantly different at $P < 0.05$ (Tukey test). A, Average fresh weight of the shoot. B, Water content calculated as follows: (fresh weight − dry weight)/fresh weight × 100 (%). C and D, Sodium (C) and potassium (D) contents of shoots. DW, Dry weight.

was significantly higher in *Thellungiella*. Consistent with earlier reports (Kawasaki et al., 2001; Taji et al., 2004), prestress-elevated or constitutive high expression of stress-relevant genes could be the basis that determines relative abiotic stress tolerance differences between plants.

Complementation by *SOS1* cDNAs of a yeast mutant lacking Na^+ transporters suggested that *ThSOS1* can function in Na^+ exclusion more efficiently than *AtSOS1*, especially at higher levels of NaCl (Fig. 2, A and B). Coexpression of AtSOS2/3 indicated that ThSOS1 was activated by Arabidopsis SOS signaling components (Fig. 2B), indicating conservation of the pathway in *Thellungiella*. However, no significant differences in Na^+/H^+ exchange rates were found in plasma membrane vesicles from cells expressing AtSOS1 or ThSOS1 (Fig. 2D). These results indicate that the two highly conserved SOS1 proteins are substantially equivalent, and the long-term effect of differential specific activity or protein abundance, too subtle to be discriminated in transport ion assays, may become amplified over time to render cells with improved salt tolerance. This is in agreement with the correlation between the salt tolerance of Arabidopsis transgenic lines and the expression level of SOS1, regardless of the origin of the protein (Fig. 3).

Sodium fluxes into and out of *Thellungiella* roots have been studied in comparison with Arabidopsis (Wang et al., 2006). A higher Na^+ efflux in the roots of Arabidopsis was reported, which partly compensated for Na^+ influx. Still, Arabidopsis plants accumulated more Na^+ than *Thellungiella* (Wang et al., 2006). Consequently, it was proposed that limitation of Na^+ influx, not higher efflux, should be the main mechanism by which *Thellungiella* could achieve lower net Na^+ accumulation under salinized conditions in com-

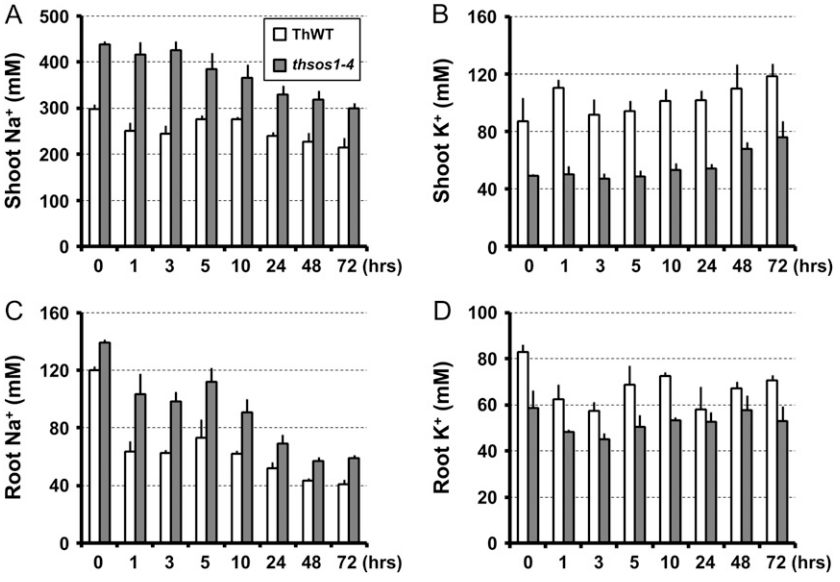

Figure 6. Comparison of Na^+ efflux characteristics between the wild type (WT) and *thsos1-4*. Hydroponically grown plants (30 d old) were subjected to stepwise increases of NaCl in growth medium to 150 mM over 2 weeks. After the removal of sodium from the medium, ion concentration in shoots and roots was monitored for 72 h. ANOVA results probing all measurements were significantly variable over time, except for the *thsos1-4* root K^+ ($P = 0.065$). A, Na^+ in shoots. B, K^+ in shoots. C, Na^+ in roots. D, K^+ in roots.

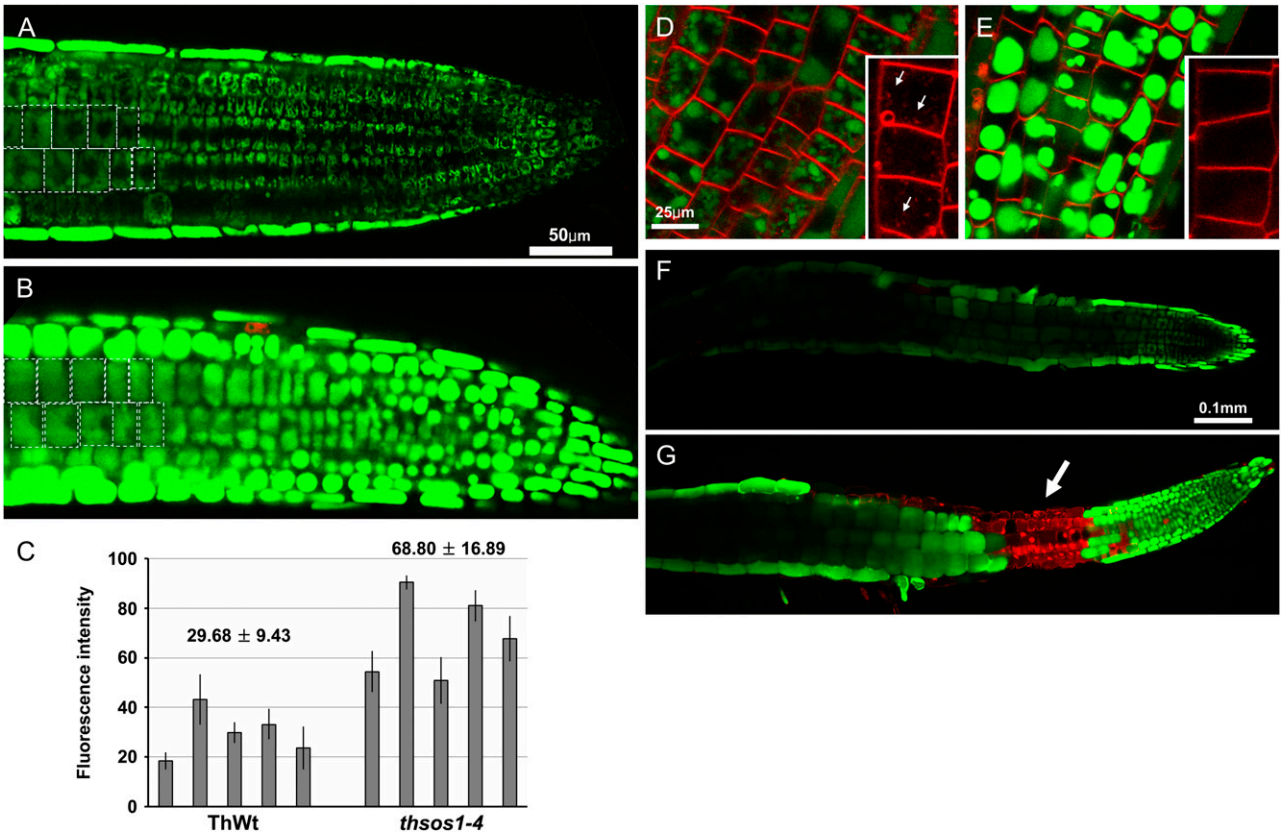

Figure 7. Imaging of Na^+ in wild-type and *thsos1-4* seedling roots. Roots of 5-d-old wild-type (A, D, and F) and *thsos1-4* (B, E, and G) seedlings were stained with CoroNa-Green AM after 24 h of 150 mM NaCl treatment and observed with a confocal microscope. A and B, Examples of CoroNa-Green staining of the root tip region. Boxes indicate the cells whose vacuolar fluorescence intensities were measured for comparison in C. C, Comparison of CoroNa-Green fluorescence intensities. Five individual plants were measured for each line. Error bars indicate SD of 10 cortex cells from each individual plant. D and E, Magnifications of A and B with FM4-64 added to visualize the membrane and endocytosis. Shown are representative images of confocal planes from surface to center at 1-μm intervals at 30 min after FM4-64 treatment. Arrows in D indicate the internalized FM4-64 dye. F and G, Confocal planes of root tip, elongation zone, and root hair zone at the plane showing epidermis and cortex cells. Propidium iodide was added to stain the damaged cells, indicated by the arrow in G.

parison with Arabidopsis. The staining by CoroNa-Green indicates Na^+ exclusion by the activity of SOS1 in specific regions of the root, rather than in all regions (Figs. 7 and 8). Thus, SOS1 may not be directly involved in plant-level Na^+ efflux but rather may function in protecting the particularly vulnerable cells of the root elongation zone (Fig. 7, F and G). Indeed, older regions of the root are not characterized by higher Na^+ content in *thsos1-4* roots, apart from the CoroNa-Green signal that indicated higher content in the xylem at later stages of salt stress (Fig. 8). The protection of the young root cells by a more abundant SOS1 in the halophyte may help to counteract Na^+ influx and, in turn, net Na^+ accumulation.

The RNAi-induced reduction of *SOS1* led to faster leaf senescence accompanied by severe shoot water loss during salt stress (Figs. 4B and 5B; Supplemental Fig. S3A). This water loss in RNAi lines was not based on impaired stomatal conductance, as the RNAi plants showed severe stress symptoms even at 100% humidity (data not shown). The phenotype was strictly Na^+ specific; the RNAi lines did not show differences compared with the wild type at K^+ concentrations up to 300 mM (Fig. 4B). The phenotype rather appeared related to the rate of Na^+ accumulation during the initial stages of exposure to high Na^+ and not to the absolute amount of Na^+ in the shoots after long-term exposure. Generally, tolerant species that have been categorized as Na^+ excluders accumulate large amounts of the ion over time, but this accumulation proceeds more slowly than in sensitive "sodium-including" species (Tester and Davenport, 2003). Indeed, Na^+ accumulation in *thsos1-4* was faster and appeared less controlled than in the wild type, which eventually contained more Na^+ than the RNAi line without adverse effects on growth at the moderate concentrations of NaCl used (Fig. 4C). Considering the positive correlation between SOS1 transcript abundance, the long-term overall high accumulation of Na^+, and the control over the rate of accumulation during

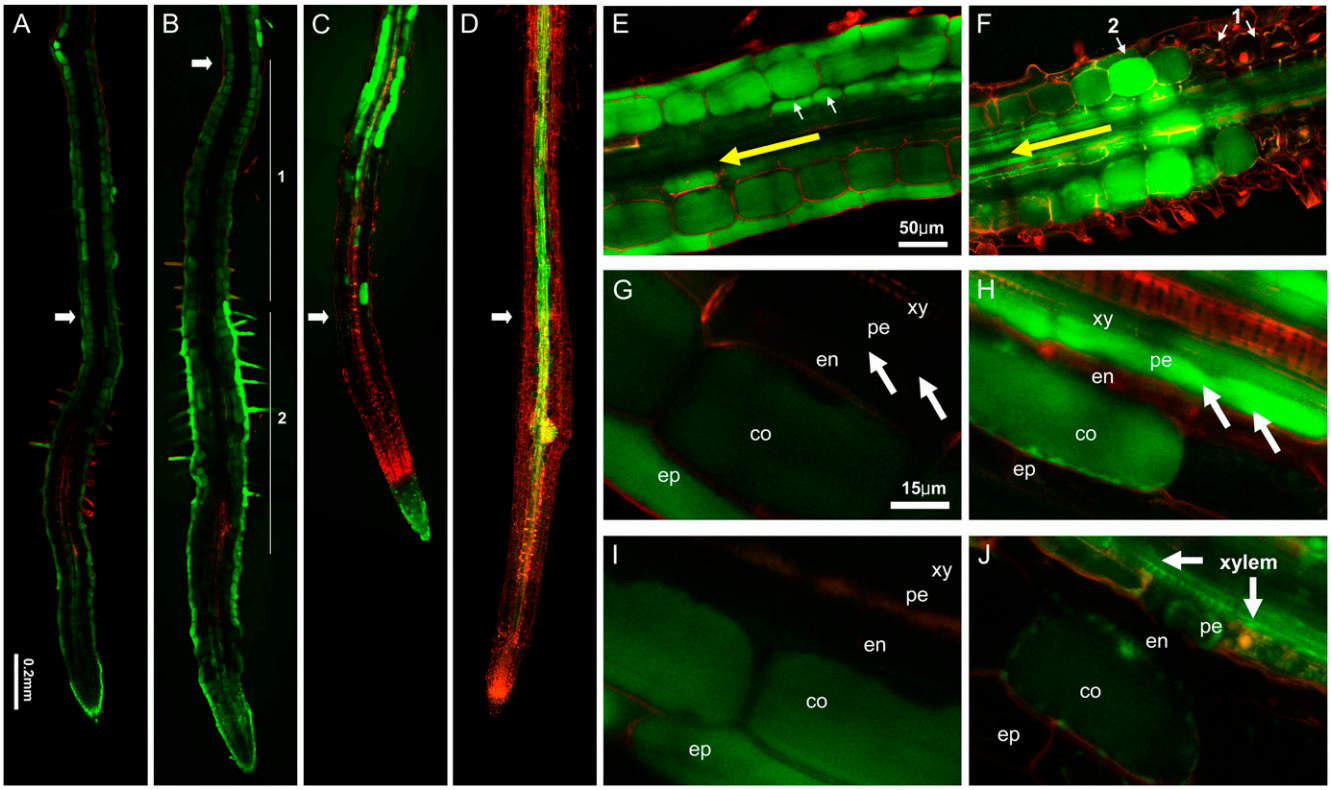

Figure 8. Localization of Na^+ in wild-type and *thsos1-4* root after prolonged stress. Shown are confocal planes of the root at the center plane stained with CoroNa-Green and propidium iodide. A to D, Arrows indicate the positions where growth under salt stress started. The wild type (A and B) and *thsos1-4* (C and D) are shown after 2 d (A and C) and 4 d (B and D) in 150 mM NaCl. E and F, Confocal plane of wild-type (E) and *thsos1-4* (F) root hair zone after 4 d in 100 mM NaCl. The yellow arrows signify the direction to the shoot. In F, arrow 1 indicates plasmolyzing cells and arrow 2 indicates higher accumulation of sodium in the adjacent cells. Both images were scanned at 25% higher gain in both channels compared with others in the figure. G to J, Confocal plane showing epidermis (ep), cortex (co), endodermis (en), pericycle (pe) layers, and xylem vessel (xy) of the wild type (G and I) and *thsos1-4* (H and J) after 2 d (G and H) or 4 d (I and J) in 150 mM NaCl.

early stages of salt stress, *Thellungiella* behaves like a true halophyte and *SOS1* expression appears to constitute an essential trait at the basis of halophytic growth. Observations of Na^+ efflux from plant tissues after removal from nonlethal concentrations of Na^+ confirmed this halophytic nature (Fig. 6). *Thellungiella* wild-type plants maintained nearly 300 mM of Na^+ in the shoot tissue even after removal of Na^+ from the medium, indicating that this halophyte might utilize ions as an osmoticum (Fig. 6A). In contrast, the higher Na^+ contents in the shoot of *thsos1-4* converged over time to the levels in wild-type shoots (Fig. 6A), indicating accumulation of Na^+ ions in *thsos1-4* shoots as an uncontrolled process requiring redistribution after the removal of external Na^+. Under very low external Na^+ (0.1, 1, and 10 mM NaCl; Supplemental Fig. S4), *thsos1-4* roots took up more Na^+ than wild-type roots after 2 h of treatment. This, together with the slower Na^+ exclusion from roots in the RNAi lines (Fig. 6C), emphasized the conserved function of *ThSOS1* in Na^+ exclusion/export under nonlethal stress conditions.

ThSOS1 Activity Leads to the Exclusion of Sodium from the Root Meristematic Region and Protects Cells of the Elongation Zone

A main objective was to observe the accumulation and distribution of Na^+ ions in cell lineages of the root, considering that we lack information on the genetic makeup that allows halophytic multicellular plants to achieve control over the rate of Na^+ accumulation. Sodium uptake was followed using the membrane-permeable fluorescent dye CoroNa-Green that binds Na^+ ions only after it has been confined within cells (Meier et al., 2006), while propidium iodide staining permitted observations of membrane integrity.

Early during salt stress, *thsos1-4* roots showed little differences when compared with the wild type in intensity or distribution of the Na^+-specific fluorescence (data not shown). Observable changes eventually originated at the root tip region, which began to show stronger fluorescence signals in *thsos1-4*, indicating SOS1's function in Na^+ exclusion (Fig. 7, A–C). Propidium iodide, which stained cell walls and dead

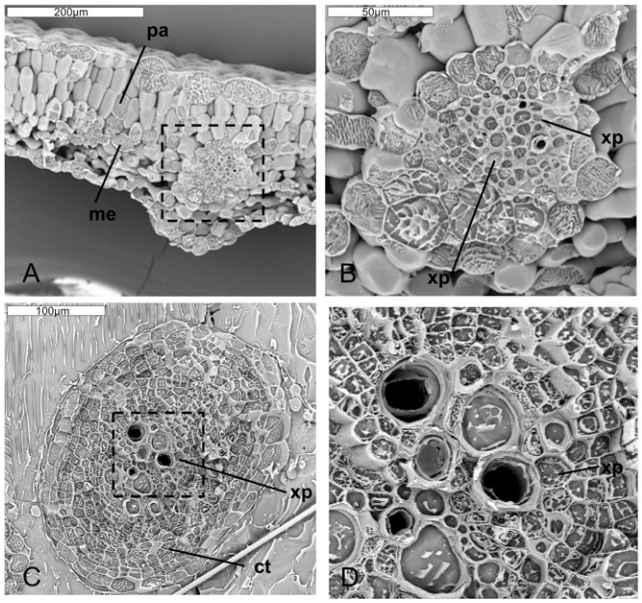

E

Organ	Cell type	Genotype	Na^+	K^+	Na^+/K^+
Leaf	pa	Wt	1.15	0.73	1.72
		thsos1-4	2.07[c]	1.13	4.84[a]
	me	Wt	1.30	0.52	2.83
		thsos1-4	2.07[b]	1.26[a]	3.17
	xp	Wt	0.44	1.21	0.53
		thsos1-4	0.78[a]	1.97[a]	0.90
Root	ct	Wt	2.08	1.79	1.65
		thsos1-4	2.17	1.36	1.86
	xp	Wt	0.80	2.11	0.55
		thsos1-4	1.89[c]	0.64[b]	6.16[b]

Figure 9. SEM-EDX analysis for ion measurement in mature plants. Wild-type (Wt) and *thsos1-4* plants were grown hydroponically for 3 weeks and treated with 250 mM NaCl for 2 d. Relative contents of K^+ and Na^+ in the indicated cell types were determined by EDX analysis as described in "Materials and Methods." A, Cross section of leaf. B, Close-up of the boxed region in A, showing central vein of leaf. C, Cross section of root. D, Close-up of the boxed region in C. Cell types identified are leaf palisade (pa), lagunar mesophyll (me), xylem parenchyma (xp), and root cortex (ct). E, Samples from both lines were processed simultaneously, and the quantitation was performed on four to six cells from each tissue type in two to three plants of each genotype. Values presented are percentages of total counts. Within pairwise comparisons, means followed by letters were statistically different at $P < 0.1$ (A), $P < 0.01$ (B), or $P < 0.001$ (C) by Fisher's LSD test.

cells, revealed that increased Na^+ fluorescence was accompanied by a gradual loss of membrane integrity, initially confined to cells of the elongation zone (Fig. 7G), spreading to cells of the root hair zone over time (Fig. 8, C and F). It appears that Na^+ exclusion by SOS1 is most critical in cells that expand and consequently take up water, whereas cells closer to the quiescent center seem to be protected by the absence of large vacuoles. These observations correspond with results from a recent study that identified the beginning of the elongation zone as the most responsive to salt stress along the longitudinal axis of the primary root (Dinneny et al., 2008). Compromised membranes may result in increased apoplastic Na^+ flux and deposition of excess (compared with the wild type) Na^+ into vacuoles, which then appeared to initiate cell death in adjacent cells, where the strongest Na^+-specific signals were typically observed (Fig. 7G). A chain reaction of cell death events accompanied the influx of Na^+ into the older part of the root as the stele began to accumulate more Na^+. This behavior of *thsos1-4* was in sharp contrast to that of wild-type plants, which confined Na^+ ions nearly exclusively to epidermis (and root cap) cells (Figs. 7F and 8, A and B). Only at concentrations higher than 350 mM NaCl in the medium did we observe the beginning deterioration of the root elongation zone in wild-type *Thellungiella*, while wild-type Arabidopsis showed this phenotype at greater than 180 mM NaCl (data not shown).

In roots incubated for an extended time (18 h) with the dye, wild-type plants showed significantly lower Na^+-specific fluorescence in cells of the pericycle and the stele (Fig. 8, E, G, and I). This visual observation matched studies using x-ray microanalysis for the localization of Na^+ in roots and confirmed the root endodermis as a major barrier controlling ion influx into the stele (Peng et al., 2004; Ottow et al., 2005). This barrier function may be important under severe stress conditions, as it has recently been reported that under moderate stress (50 mM NaCl) this role appears to be satisfied by cells of the epidermis and cortex of wheat (*Triticum aestivum*; Läuchli et al., 2008). In strong contrast, the localization of Na^+ and cell viability staining in *thsos1-4* roots clearly revealed higher uptake into the root vasculature (Fig. 8, F, H, and J) and greater movement most likely to the shoot under transpiring conditions. This identifies the crucial barrier at the pericycle/endodermis boundary, where indeed Arabidopsis showed strong expression of *SOS1* in a construct expressing *GUS* under control of the *AtSOS1* promoter (Shi et al., 2002). Interestingly, the appearance of Na^+ ion-specific fluorescence inside the pericycle of *thsos1-4* occurred at the same time as root tip damage, suggesting that the protection of root tips by SOS1 may also contribute to the protection of the root stele from the intrusion of Na^+ ions. SEM-EDX analysis on roots of mature plants confirmed higher accumulation of Na^+ in the root stele and cells of the photosynthetic tissues of *thsos1-4* (Fig. 9), as observed by measuring ion contents (Figs. 5C and 6A) and monitoring Na^+-specific fluorescence (Fig. 8) in younger plants.

ThSOS1, Endocytosis Protection, and Halophytic Adaptation

New evidence has revealed SOS1 and the SOS pathway with a function not only as a Na^+ exporter but as a mediator of intracellular Ca^{2+} and pH homeostasis (Cheng et al., 2004; Shabala et al., 2005). Involve-

ment of SOS1 in regulating ROS metabolism through an interaction with RCD1, involved in radical-based signaling, through its long C-terminal cytoplasmic tail has been reported (Katiyar-Agarwal et al., 2006). Mutations in SOS1 and other SOS pathway components are known to affect aspects of root development, such as cortical microtubule organization and gravitropism (Sun et al., 2008) under salt stress. Considering the negative effect on endocytosis by a suppression of ThSOS1 expression, indicated by the abolishment of FM4-64 import in *thsos1-4* root cells (Fig. 7E), protection of endocytosis may be suggested as an additional role of *SOS1*. In Arabidopsis, SOS1 affects cortical microtubule organization and endocytic vesicles are known to be transported along actin filaments and microtubules (Shoji et al., 2006; Soldati and Schliwa, 2006). In affecting endocytosis under salinity conditions, a lack of *SOS1* could also interfere with other functions of endocytosis, including polar auxin transport (Dhonukshe et al., 2007), brassinosteroid signaling (Geldner et al., 2007), recycling of plasma membrane receptors and ion channels (Murphy et al., 2005; Sutter et al., 2007), and cytokinesis (Dhonukshe et al., 2006; Reichardt et al., 2007), and therefore result in the termination of root growth and cell death (Fig. 7F). SOS1 may be involved in endocytosis via the yet unknown interaction with a component or regulator of intracellular trafficking or via an indirect pathway including the regulation of cytosolic or vacuolar pH under salt stress (Shabala et al., 2005), which may then affect endomembrane and vesicle trafficking (Li et al., 2005; Shoji et al., 2006).

SOS1 activity could protect endocytosis of cells in the root tip and elongation zone and ultimately sustain membrane integrity, thus providing an essential stopgap measure or temporary protective solution allowing for other defensive measures to become established in the plants. Supporting this view is the fact that cells in *Thellungiella* wild-type roots that developed after the plants had adapted to increased salinity showed a stronger fluorescence than cells that developed during the stress imposition period (Fig. 8B, compare areas 1 and 2). Apparently, the halophyte achieved adaptation in newly developed root cells within less than 2 d, which was absent from *thsos1-4* roots that suffered extensive damage, cell death, and uncontrolled apoplastic Na^+ influx into the root stele and shoot (Fig. 8D). Stress "preparedness" by *Thellungiella* seems to extend to other functions, because the plant contains, compared with Arabidopsis, higher amounts of metabolites, including Pro, trehalose, inositols, and several organic acids and substantially unique yet unknown compounds (Taji et al., 2004; Gong et al., 2005; Oh et al., 2007) that are additionally salt stress inducible. Although Arabidopsis shows induction, often stronger than *Thellungiella*, for a number of putatively protective pathways, the ultimate accumulation of metabolites achieved by Arabidopsis is less than that seen in *Thellungiella* (Gong et al., 2005). Similarly, *thsos1-4* shared with Arabidopsis the absence of drastically increased levels of metabolites (Oh et al., 2007). By providing a temporal barrier to a sudden exposure to high Na^+ in the root cell elongation zone, *ThSOS1* prohibited the onset of a chain reaction leading to cell death and apoplastic Na^+ influx into the shoots. *ThSOS1* activity then resulted in adaptation of the entire plant, allowing higher levels of sodium accumulation in the shoot to be nontoxic.

MATERIALS AND METHODS

Transformation of Yeast and Plants

Transformation and salt treatment of yeast AXT3K mutant and Arabidopsis (*Arabidopsis thaliana* Columbia wild type) were performed as described (Shi et al., 2003; Martinez-Atienza et al., 2007) using the full-length *ThSOS1* cDNA (accession no. EF207775). Transgenic Arabidopsis lines expressing *AtSOS1* (lines 1-1 and 7-1) were kind gifts from Dr. Huazhong Shi (Shi et al., 2003). *Thellungiella salsuginea* expressing *ThSOS1* RNAi were developed as described by Oh et al. (2007).

Plant Growth and Stress Treatment

All plants were grown under 14-h-day and 10-h-night conditions. For the assessment of salt tolerance of Arabidopsis expressing *ThSOS1* and *AtSOS1*, seedlings were transferred to medium containing 200 mM NaCl as described (Shi et al., 2003). Except when indicated otherwise, seedlings were grown on quarter-strength Murashige and Skoog medium supplemented with 2% Suc and 0.8% Select-Agar (Invitrogen), with the petri dish sealed using porous Micropore tape. For root growth assay, 10-d-old seedlings were transferred to medium containing various concentrations of NaCl with the plates oriented vertically. Salt treatment of mature plants was performed as described (Oh et al., 2007).

Transcript Level

All analyses used pools of 10 plants for each sample. For the interspecific comparison, 2-week-old (for Arabidopsis) or 3-week-old (for *Thellungiella*) plants, thus accounting for identical growth stage (Gong et al., 2005), were incubated on vertical plates containing salt for 12 h, and their tissues were pooled and harvested for RNA extraction and RT-PCR analyses. Quantitative real-time PCR results were normalized to ACT2 gene expression. For the list of primers used, see Supplemental Table S1.

Ion Measurements

For measurement of ion contents in the seedling shoot, medium containing 200 mM NaCl was placed in single compartments of a half-divided petri dish. Two-week-old seedlings were grown vertically with their shoot placed in the empty compartment not contacting the medium. Harvested shoot samples were dried, dissolved in HNO_3, and analyzed by inductively coupled plasma-optical emission spectrometry (Optima 2000; Perkin-Elmer). For measurement of ion contents in hydroponically grown plants, atomic absorption spectrophotometry (Perkin-Elmer 1100B) was applied to saps extracted from leaf and root frozen samples as described (Gorham et al., 1994).

SEM-EDX was used on frozen sections of leaves and roots harvested from 3-week-old hydroponically grown plants. Samples were mounted in slots of copper holders, fixed with OCT Compound (BDH), and dipped into a bath of slush nitrogen prior to transfer under vacuum into the cryopreparation chamber (CT1500; Oxford Instruments) attached to the scanning electron microscope (DSM 960; Zeiss). The chamber temperature was left to rise from −163°C to −90°C and set for 10 min for ice sublimation before sputter coating with gold (2 min). Samples were analyzed with an ATW detector interfaced with a Link ISIS analyzer (Oxford Instruments) under the following conditions: accelerating voltage, 15 kV; takeoff angle, 42°C; collecting time of x-ray counts, 100 s; working distance between sample and detector, 24 mm. Measurements were performed by focusing on exposed vacuoles of specific cells.

Ion Transport Assays

Vesicles of the yeast plasma membrane were produced by two-phase partitioning as described previously (Martinez-Atienza et al., 2007). The purity of vesicle preparations was tested by measuring ATP hydrolysis in the presence of inhibitors of mitochondrial (azide), vacuolar (nitrate), and plasmalemma (vanadate) ATPases. The relative sensitivity of total ATPase activity to these inhibitors demonstrated that vesicle preparations were highly enriched in the plasma membrane. Na^+/H^+ exchange was monitored by the quinacrine fluorescence quenching method. An inside-acid proton gradient (ΔpH) across vesicle membranes was established after the addition of ATP. NaCl was added once ΔpH reached a steady state, and fluorescence recovery (i.e. dissipation of the ΔpH) was recorded with a fluorescence spectrophotometer (Hitachi F-2500). To determine initial rates of Na^+/H^+ exchange, the change of relative fluorescence was measured 30 s after the addition of sodium salts. Specific activity was calculated by dividing the initial rate of fluorescence recovery, expressed as a ratio of the preformed pH gradient, by the mass of plasma membrane protein in the reaction and time ($\Delta F\ mg^{-1}\ min^{-1}$, where $\Delta F = F_{30} - F_0/F_{max} - F_{min}$). The change of pH value was measured at excitation and emission wavelengths of 430 and 500 nm, respectively.

Visualization of Na^+ Ions

One week-old seedlings were stained and observed by confocal microscopy (TCS SP2 RBB; Leica) after salt treatment on medium containing 1.1% type A agar (Sigma-Aldrich). Staining to reveal Na^+ content was performed as described (Mazel et al., 2004; Leshem et al., 2006; Meier et al., 2006). Roots were either stained with 20 μM CoroNa-Green AM (Invitrogen) in the presence of a final concentration of 0.02% pluronic acid (Invitrogen) for 3 h or incubated on a filter paper soaked with medium containing 10 μM CoroNa-Green for 18 h to stain the Na^+ in the root stele. For visualizing the stele of roots, fluorescein diacetate (Invitrogen) replaced CoroNa-Green AM in some experiments as positive controls of dye penetration. Where indicated, 2.5 $\mu g\ mL^{-1}$ propidium iodide (Invitrogen) or 5 μM FM4-64 (Invitrogen) was added after incubation with CoroNa-Green AM.

Supplemental Data

The following materials are available in the online version of this article.

Supplemental Figure S1. Phylogenic relationships of SOS1 homologs from various species.

Supplemental Figure S2. Comparison of *SOS1* mRNA abundance in mature Arabidopsis and *Thellungiella* plants.

Supplemental Figure S3. Phenotypes of mature *ThSOS1* RNAi plants.

Supplemental Figure S4. Comparison of sodium uptake under mildly saline conditions.

Supplemental Figure S5. Relative *SOS1* mRNA levels in the seedling roots used for microscopy.

Supplemental Figure S6. Confocal planes of CoroNa-Green staining of the root tip region under salt stress.

Supplemental Table S1. List of RT-PCR primers.

ACKNOWLEDGMENTS

We thank Drs. Qingqui Gong, Shisong Ma, and Valeriy Poroyko for discussions and Drs. Francoise Quigley and Valeriy Poroyko for *Thellungiella* SOS1 cDNAs.

Received February 28, 2009; accepted June 27, 2009; published July 1, 2009.

LITERATURE CITED

Adams P, Nelson DE, Yamada S, Chmara W, Jensen RG, Bohnert HJ, Griffiths H (1998) Growth and development of *Mesembryanthemum crystallinum* (Aizoaceae). New Phytol **138:** 171–190

Amtmann A (2009) Learning from evolution: *Thellungiella* generates new knowledge on essential and critical components of abiotic stress tolerance in plants. Mol Plant **2:** 3–12

Berthomieu P, Conejero G, Nublat A, Brackenbury WJ, Lambert C, Savio C, Uozumi N, Oiki S, Yamada K, Cellier F, et al (2003) Functional analysis of AtHKT1 in *Arabidopsis* shows that Na^+ recirculation by the phloem is crucial for salt tolerance. EMBO J **22:** 2004–2014

Bressan RA, Zhang C, Zhang H, Hasegawa PM, Bohnert HJ, Zhu JK (2001) Learning from the Arabidopsis experience: the next gene search paradigm. Plant Physiol **127:** 1354–1360

Cheng NH, Pittman JK, Zhu JK, Hirschi KD (2004) The protein kinase SOS2 activates the *Arabidopsis* H^+/Ca^{2+} antiporter CAX1 to integrate calcium transport and salt tolerance. J Biol Chem **279:** 2922–2926

Chinnusamy V, Zhu J, Zhu JK (2006) Salt stress signaling and mechanisms of plant salt tolerance. Genet Eng (N Y) **27:** 141–177

Chung JS, Zhu JK, Bressan RA, Hasegawa PM, Shi H (2008) Reactive oxygen species mediate Na^+-induced *SOS1* mRNA stability in *Arabidopsis*. Plant J **53:** 554–565

Czechowski T, Stitt M, Altmann T, Udvardi MK, Scheible WR (2005) Genome-wide identification and testing of superior reference genes for transcript normalization in Arabidopsis. Plant Physiol **139:** 5–17

Davenport R, James RA, Zakrisson-Plogander A, Tester M, Munns R (2005) Control of sodium transport in durum wheat. Plant Physiol **137:** 807–818

Demidchik V, Maathuis FJ (2007) Physiological roles of nonselective cation channels in plants: from salt stress to signalling and development. New Phytol **175:** 387–404

Dhonukshe P, Aniento F, Hwang I, Robinson DG, Mravec J, Stierhof YD, Friml J (2007) Clathrin-mediated constitutive endocytosis of PIN auxin efflux carriers in *Arabidopsis*. Curr Biol **17:** 520–527

Dhonukshe P, Baluska F, Schlicht M, Hlavacka A, Samaj J, Friml J, Gadella TW Jr (2006) Endocytosis of cell surface material mediates cell plate formation during plant cytokinesis. Dev Cell **10:** 137–150

Dinneny JR, Long TA, Wang JY, Jung JW, Mace D, Pointer S, Barron C, Brady SM, Schiefelbein J, Benfey PN (2008) Cell identity mediates the response of *Arabidopsis* roots to abiotic stress. Science **320:** 942–945

Essah PA, Davenport R, Tester M (2003) Sodium influx and accumulation in Arabidopsis. Plant Physiol **133:** 307–318

Geldner N, Hyman DL, Wang X, Schumacher K, Chory J (2007) Endosomal signaling of plant steroid receptor kinase BRI1. Genes Dev **21:** 1598–1602

Gong Q, Li P, Ma S, Indu Rupassara S, Bohnert HJ (2005) Salinity stress adaptation competence in the extremophile *Thellungiella halophila* in comparison with its relative *Arabidopsis thaliana*. Plant J **44:** 826–839

Gorham J, Papa R, Aloy-Lleonart M (1994) Varietal differences in sodium uptake in barley cultivars exposed to soil salinity or salt spray. J Exp Bot **45:** 895–901

Hasegawa PM, Bressan RA, Zhu JK, Bohnert HJ (2000) Plant cellular and molecular responses to high salinity. Annu Rev Plant Physiol Plant Mol Biol **51:** 463–499

Inan G, Zhang Q, Li P, Wang Z, Cao Z, Zhang H, Zhang C, Quist TM, Goodwin SM, Zhu J, et al (2004) Salt cress: a halophyte and cryophyte Arabidopsis relative model system and its applicability to molecular genetic analyses of growth and development of extremophiles. Plant Physiol **135:** 1718–1737

Katiyar-Agarwal S, Zhu J, Kim K, Agarwal M, Fu X, Huang A, Zhu JK (2006) The plasma membrane Na^+/H^+ antiporter SOS1 interacts with RCD1 and functions in oxidative stress tolerance in *Arabidopsis*. Proc Natl Acad Sci USA **103:** 18816–18821

Kawasaki S, Borchert C, Deyholos M, Wang H, Brazille S, Kawai K, Galbraith D, Bohnert HJ (2001) Gene expression profiles during the initial phase of salt stress in rice. Plant Cell **13:** 889–905

Läuchli A, James RA, Huang CX, McCully M, Munns R (2008) Cell-specific localization of Na^+ in roots of durum wheat and possible control points for salt exclusion. Plant Cell Environ **31:** 1565–1574

Leshem Y, Melamed-Book N, Cagnac O, Ronen G, Nishri Y, Solomon M, Cohen G, Levine A (2006) Suppression of Arabidopsis vesicle-SNARE expression inhibited fusion of H_2O_2-containing vesicles with tonoplast and increased salt tolerance. Proc Natl Acad Sci USA **103:** 18008–18013

Li J, Yang H, Peer WA, Richter G, Blakeslee J, Bandyopadhyay A, Titapiwantakun B, Undurraga S, Khodakovskaya M, Richards EL, et al (2005) *Arabidopsis* H^+-PPase AVP1 regulates auxin-mediated organ development. Science **310:** 121–125

Lunde C, Drew DP, Jacobs AK, Tester M (2007) Exclusion of Na^+ via

sodium ATPase (PpENA1) ensures normal growth of *Physcomitrella patens* under moderate salt stress. Plant Physiol **144:** 1786–1796

Martinez-Atienza J, Jiang X, Garciadeblas B, Mendoza I, Zhu JK, Pardo JM, Quintero FJ (2007) Conservation of the salt overly sensitive pathway in rice. Plant Physiol **143:** 1001–1012

Mazel A, Leshem Y, Tiwari BS, Levine A (2004) Induction of salt and osmotic stress tolerance by overexpression of an intracellular vesicle trafficking protein AtRab7 (AtRabG3e). Plant Physiol **134:** 118–128

Meier SD, Kovalchuk Y, Rose CR (2006) Properties of the new fluorescent Na^+ indicator CoroNa Green: comparison with SBFI and confocal Na^+ imaging. J Neurosci Methods **155:** 251–259

Munns R, James RA, Lauchli A (2006) Approaches to increasing the salt tolerance of wheat and other cereals. J Exp Bot **57:** 1025–1043

Murphy AS, Bandyopadhyay A, Holstein SE, Peer WA (2005) Endocytotic cycling of PM proteins. Annu Rev Plant Biol **56:** 221–251

Oh DH, Gong Q, Ulanov A, Zhang Q, Li Y, Ma W, Yun DJ, Bressan RA, Bohnert HJ (2007) Sodium stress in the halophyte *Thellungiella halophila* and transcriptional changes in a *thsos1*-RNA interference line. J Integr Plant Biol **49:** 1484–1496

Ottow EA, Brinker M, Teichmann T, Fritz E, Kaiser W, Brosche M, Kangasjarvi J, Jiang X, Polle A (2005) *Populus euphratica* displays apoplastic sodium accumulation, osmotic adjustment by decreases in calcium and soluble carbohydrates, and develops leaf succulence under salt stress. Plant Physiol **139:** 1762–1772

Pardo JM, Cubero B, Leidi EO, Quintero FJ (2006) Alkali cation exchangers: roles in cellular homeostasis and stress tolerance. J Exp Bot **57:** 1181–1199

Peng YH, Zhu YF, Mao YQ, Wang SM, Su WA, Tang ZC (2004) Alkali grass resists salt stress through high $[K^+]$ and an endodermis barrier to Na^+. J Exp Bot **55:** 939–949

Qiu QS, Guo Y, Dietrich MA, Schumaker KS, Zhu JK (2002) Regulation of SOS1, a plasma membrane Na^+/H^+ exchanger in *Arabidopsis thaliana*, by SOS2 and SOS3. Proc Natl Acad Sci USA **99:** 8436–8441

Quintero FJ, Ohta M, Shi H, Zhu JK, Pardo JM (2002) Reconstitution in yeast of the *Arabidopsis* SOS signaling pathway for Na^+ homeostasis. Proc Natl Acad Sci USA **99:** 9061–9066

Reichardt I, Stierhof YD, Mayer U, Richter S, Schwarz H, Schumacher K, Jurgens G (2007) Plant cytokinesis requires *de novo* secretory trafficking but not endocytosis. Curr Biol **17:** 2047–2053

Ren ZH, Gao JP, Li LG, Cai XL, Huang W, Chao DY, Zhu MZ, Wang ZY, Luan S, Lin HX (2005) A rice quantitative trait locus for salt tolerance encodes a sodium transporter. Nat Genet **37:** 1141–1146

Rus A, Lee BH, Munoz-Mayor A, Sharkhuu A, Miura K, Zhu JK, Bressan RA, Hasegawa PM (2004) AtHKT1 facilitates Na^+ homeostasis and K^+ nutrition in planta. Plant Physiol **136:** 2500–2511

Shabala L, Cuin TA, Newman IA, Shabala S (2005) Salinity-induced ion flux patterns from the excised roots of *Arabidopsis sos* mutants. Planta **222:** 1041–1050

Shi H, Ishitani M, Kim C, Zhu JK (2000) The *Arabidopsis thaliana* salt tolerance gene *SOS1* encodes a putative Na^+/H^+ antiporter. Proc Natl Acad Sci USA **97:** 6896–6901

Shi H, Lee BH, Wu SJ, Zhu JK (2003) Overexpression of a plasma membrane Na^+/H^+ antiporter gene improves salt tolerance in *Arabidopsis thaliana*. Nat Biotechnol **21:** 81–85

Shi H, Quintero FJ, Pardo JM, Zhu JK (2002) The putative plasma membrane Na^+/H^+ antiporter SOS1 controls long-distance Na^+ transport in plants. Plant Cell **14:** 465–477

Shoji T, Suzuki K, Abe T, Kaneko Y, Shi H, Zhu JK, Rus A, Hasegawa PM, Hashimoto T (2006) Salt stress affects cortical microtubule organization and helical growth in *Arabidopsis*. Plant Cell Physiol **47:** 1158–1168

Soldati T, Schliwa M (2006) Powering membrane traffic in endocytosis and recycling. Nat Rev Mol Cell Biol **7:** 897–908

Sun F, Zhang W, Hu H, Li B, Wang Y, Zhao Y, Li K, Liu M, Li X (2008) Salt modulates gravity signaling pathway to regulate growth direction of primary roots in Arabidopsis. Plant Physiol **146:** 178–188

Sutter JU, Sieben C, Hartel A, Eisenach C, Thiel G, Blatt MR (2007) Abscisic acid triggers the endocytosis of the *Arabidopsis* KAT1 K^+ channel and its recycling to the plasma membrane. Curr Biol **17:** 1396–1402

Taji T, Seki M, Satou M, Sakurai T, Kobayashi M, Ishiyama K, Narusaka Y, Narusaka M, Zhu JK, Shinozaki K (2004) Comparative genomics in salt tolerance between Arabidopsis and Arabidopsis-related halophyte salt cress using Arabidopsis microarray. Plant Physiol **135:** 1697–1709

Tester M, Davenport R (2003) Na^+ tolerance and Na^+ transport in higher plants. Ann Bot (Lond) **91:** 503–527

Vera-Estrella R, Barkla BJ, Garcia-Ramirez L, Pantoja O (2005) Salt stress in *Thellungiella halophila* activates Na^+ transport mechanisms required for salinity tolerance. Plant Physiol **139:** 1507–1517

Volkov V, Amtmann A (2006) *Thellungiella halophila*, a salt-tolerant relative of *Arabidopsis thaliana*, has specific root ion-channel features supporting K^+/Na^+ homeostasis under salinity stress. Plant J **48:** 342–353

Wang B, Davenport RJ, Volkov V, Amtmann A (2006) Low unidirectional sodium influx into root cells restricts net sodium accumulation in *Thellungiella halophila*, a salt-tolerant relative of *Arabidopsis thaliana*. J Exp Bot **57:** 1161–1170

Yamaguchi T, Aharon GS, Sottosanto JB, Blumwald E (2005) Vacuolar Na^+/H^+ antiporter cation selectivity is regulated by calmodulin from within the vacuole in a Ca^{2+}- and pH-dependent manner. Proc Natl Acad Sci USA **102:** 16107–16112